

Influence of Cell Design and Electrode Materials on the Decolouration of Dyeing Effluents

M. Sala^{1,*}, A.I. del Río², J. Molina², F. Cases², M.C. Gutiérrez-Bouzán¹

¹ INTEXTER, Institut d'Investigació Tèxtil i Cooperació Industrial de Terrassa; UPC, Universitat Politècnica de Catalunya; Colom 15, 08222 Terrassa, Spain.

² Departamento de Ingeniería Textil y Papelera, Escuela Politécnica Superior Alcoy. UPV, Universitat Politècnica de València; Plaza Ferrándiz y Carbonell, s/n 03801 Alcoy, Spain

*E-mail: mireia.sala@intexter.upc.edu

Received: 25 July 2012 / Accepted: 23 October 2012 / Published: 1 December 2012

Electrochemical techniques are applied in different textile processes, including wastewater treatment, as they are clean and generally operate at room temperature. In the current work, doped SnO₂ electrodes (Ti/SnO₂-Sb-Pt) were prepared. They were used as anodes in two electrochemical cells (simple batch mode and batch recirculation mode) to achieve the removal of two reactive azo dyes (Remazol Black 133B and Procion Yellow H-EXL) in synthetic dyeing effluents. With these electrodes, both cells exhibit similar decolouration rates. In addition, the doped SnO₂ electrodes are compared with Ti/Pt electrodes in order to establish the influence of electrode material. They were applied to the treatment of four synthetic effluents containing one of the following reactive azo dyes: Remazol Black 133B, Procion Yellow H-EXL, Procion Crimson H-EXL and Procion Navy H-EXL. It was stated that the decolouration is faster with Ti/Pt anodes than with the doped SnO₂ ones, but these last electrodes generate lower amount of chloroform during the electrolysis.

Keywords: Electrochemical treatment, oxidation-reduction process, reactive dyes decolouration, cell design, electrode material.

1. INTRODUCTION

Traditionally, the electrochemical techniques were used for the synthesis of compounds or for metal recovery treatments. But more recently, a wide range of other applications have been proposed, some of them including the textile industry. It is possible to find the application of these techniques in several textile processes [1] like bleaching of fabrics (indigo denims or fibres), sulphur and vat dyeing or even in manufacturing of polymers. There are also some increasing tendencies in producing smart

textiles using conductive polymers to obtain a textile with specific property, but the wider range of applications is related to colour removal in wastewater treatments.

In textile industry, coloured wastewaters are produced in dyeing and finishing processes. Reactive dyes are commonly used in cotton industry. Their low degree of exhaustion increases the problem of the high coloured effluents. Moreover these kinds of dyes are only partially removed under aerobic conditions in the biological plants. The application of additional treatments to remove colour in this type of wastewater is required in order to accomplish with current regulations.

Different methods are used to achieve effective colour removal of wastewaters. Physico-chemical methods are based on the dye separation from the solution, which involve a tertiary treatment to destroy the concentrated dye. In addition, adsorbents materials (active carbon [2-4], silica gel and alumina) have to be regenerated after some treatments [5]. Filtration and the use of membranes (mainly nano-membranes [6-7]) require cleaning treatments, whereas flocculation-coagulation methods [8] produce sludge. The dye degradation by an enzymatic method requires further investigation in order to know which enzymatic process takes place [9]; also both temperature and pressure parameters have to be controlled to avoid enzyme denaturalization. Chemical oxidation methods such as ozonation [10, 11] or Fenton processes [12, 13] are quite expensive and the addition of auxiliary chemicals is necessary which can involve operational difficulties [14,15]. Biological treatments are the simplest methods but do not supply efficient decolouration results because of their chemical stability and resistance to microbiological attack [16]. Consequently, nowadays electrochemical methods are being the focus of different research studies on wastewater decolouration treatments [9, 14, 16-19]. The advantages of these techniques are that operation at smooth conditions is possible and they use electron as a clean reagent. They also provide versatility, high energy efficiency, safety and ease for automation [17].

A.I. del Río et al. studied the efficiency of electrochemical treatment with DSA in both a divided cell (for oxidation and reductions processes separately) [20] and an undivided cell (oxido-reduction processes). The highest decolouration rates were obtained with the second process [21]. According to those results, the studies carried out in the current paper were focused on an oxido-reduction process in an undivided cell.

In this work, electrodes made of Ti/SnO₂-Sb-Pt were synthesized. These electrodes demonstrated to be useful for dyeing wastewater treatments. They have higher electroactivity and service life than Ti/SnO₂ and Ti/SnO₂-Sb electrodes [22]. The Ti/SnO₂-Sb-Pt electrodes were used as anode in two electrochemical cells for the treatment of synthetic coloured effluents containing two reactive dyes to achieve their colour removal. Decolouration efficiency with the two cell designs was studied to evaluate the influence of the cell design in the decontamination of these kinds of effluents.

Due to its simplicity, the simple batch cell was selected to carry out the study on the electrode material influence. As the two dyes selected in the first part showed different behaviour, the second section was performed with two additional dyes. Therefore, four synthetic coloured effluents, each of them containing a different reactive dye, were treated at the same conditions using active electrodes made of Ti/Pt and the doped SnO₂ electrodes (Ti/SnO₂-Sb-Pt) previously prepared.

Reactive azo dyes were selected for the study because they represent about 20-30% of the total market [23] and more of 50% the cotton market. Their structure contains a reactive group which reacts

with the fibre and a chromophore group which causes the colour. The chromophore group azo (-N=N-) represents about the 65% of worldwide dye production [24-27].

The dye degradation was followed by mean of a UV-Visible spectrophotometer, by recording the absorbance decrease at its maximum wavelength. CGMS analyses were carried out on the final treated samples in order to evaluate the generation of volatile halogenated compounds during the electrolysis.

2. EXPERIMENTAL

2.1. Preparation of the doped SnO₂ electrodes (Ti/SnO₂-Sb-Pt).

The doped SnO₂ electrodes (Ti/SnO₂-Sb-Pt) were synthesized by a thermal decomposition method of the precursor solution in a titanium substrate [28-32]. The initial titanium electrodes with an area of 48.8cm² approximately, were pre-treated with acetone in the ultrasounds bath for 10min. This treatment is based on the elimination of the superficial layer of TiO₂ (an electric semiconductor) which gives to the electrodes a higher roughness that improves the electrocatalytic oxide adherence. Then the titanium supports were treated in a boiling solution of oxalic acid (10%) for 1 hour. Subsequently the supports were washed up with ultrapure water and the precursor solution was applied with a brush (the precursor solution is a mixture of: 10% SnCl₄·5H₂O, provided by Aldrich + 1% SbCl₃, from Fluka + 0.252% H₂PtCl₆·6H₂O, supplied by Merck; in a dilution of ethanol + HCl provided by Panreac and Merck, respectively). After that, the electrodes were placed into an oven at 400°C for 10min. This action is repeated successively until a 2mg/cm² of weight increment was obtained. During this treatment the precursor salt solution was decomposed and the metal oxide was formed. Finally, a thermal treatment at 600°C was applied for 1hour.

2.2. Dyes and dyeing reagents

Table 1. Description of selected Reactive Dyes

Abbreviation	Commercial Name	C.I. Name	Chromophore	Reactive group	λ_{\max} (nm)
RB5	Remazol Black 133B	Reactive Black 5	Diazo	Sulphatoethylsulfone	600
PY	Procion Yellow H-EXL	Reactive Yellow 138:1	Diazo	Monochlorotriazine	416
PC	Procion Crimson H-EXL	Reactive Red 231	Diazo	Monochlorotriazine	545
PN	Procion Navy H-EXL	Not registred	Diazo	Monochlorotriazine	606

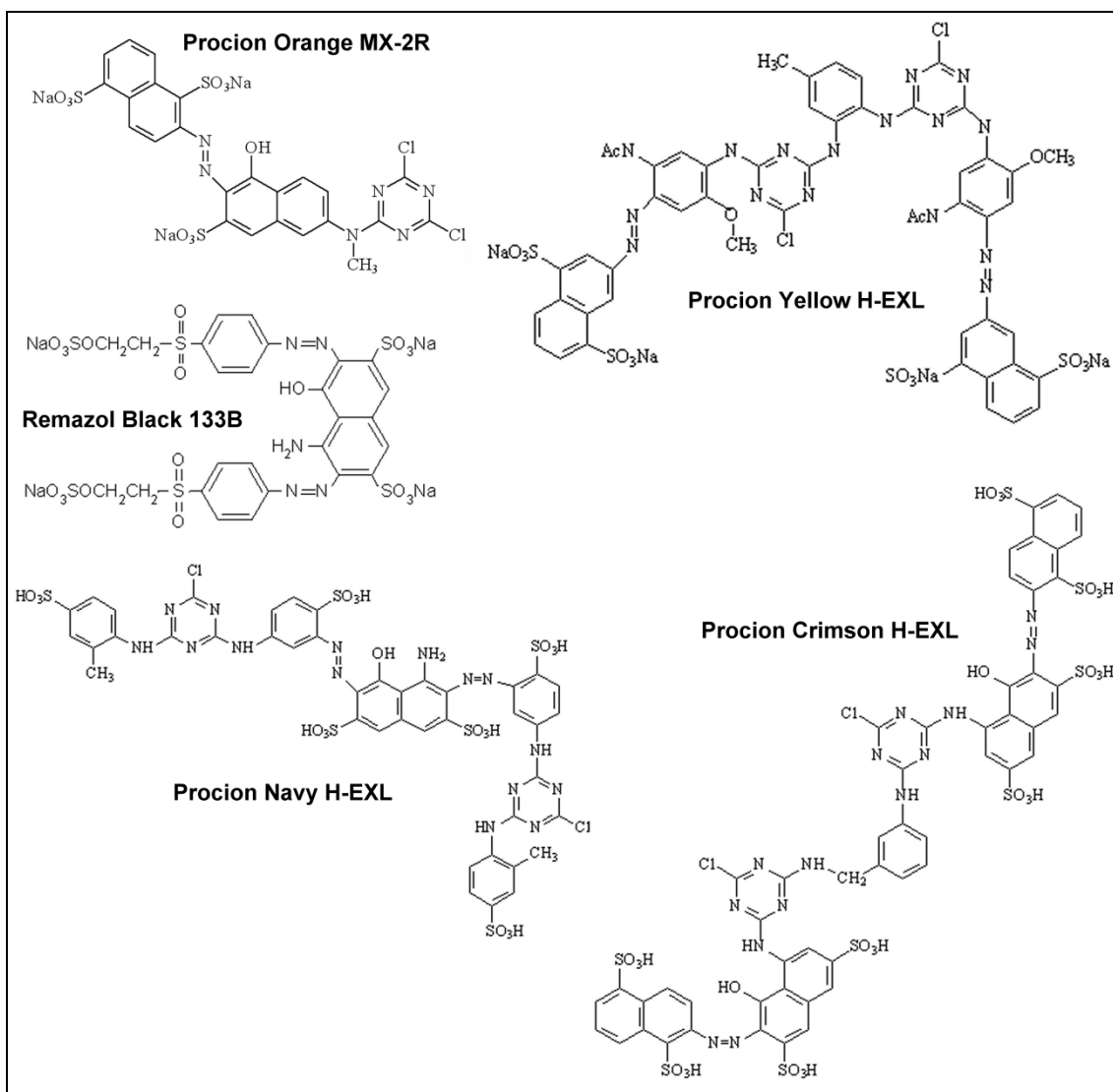


Figure 1. Chemical structure of the selected dyes

Four reactive dyes, kindly provided by DyStar, were selected. Their name and functional groups are listed in Table 1. Figure 1 shows their chemical structure. As it can be seen, all of them have two reactive groups. Birreactive dyes are widely used nowadays due to their higher dyeing exhaustion values with respect to monoreactive dyes.

The chemical products used in the effluents preparation (NaOH , Na_2SO_4 , and NaCl) were supplied by Merck and Fluka (analysis quality). The p-bromofluorobenzene used as Internal Standard in the gas chromatography analysis was provided by AccuStandard (chromatography grade).

2.3. Effluent preparation

Dyebath effluents with reactive dyes were prepared in the laboratory to simulate the coloured industrial effluents. During the dyeing process, the dye which does not react with the fibre remains

hydrolyzed in the bath solution. In this situation, the chlorine atoms of the dye molecule are replaced by two OH groups. These hydrolyzed reactive dyes are the responsible of the textile effluents colour. The pH effect is not studied because the dyeing effluents with reactive dyes are very alkali and with high salinity. Taking into account an environmental point of view, modify the pH of these effluents is not advisable due to the salinity increasing.

In the first part of the study (cell design comparison) the dye concentration was 0.8g/L, the treated volume was 0.45L for the batch recirculation mode cell and 2L for the simple batch mode cell (the specific volume of each cell). In the second part (electrodes comparison), the electrolysis was carried out in the simple batch mode cell (volume 2L) at 0.1g/L dye concentration. A small amount of sodium chloride (0.3g/L) was added to obtain the same chloride concentration than the decalcified water (used in the industrial processes). Different dye and chloride concentrations were selected for each study. In the first case, slow decolouration rates were required to demonstrate the cell design influence, as it was not expected to be the most determining factor in the decolouration. In the second case, the electrode material was expected to be an important factor in dyes decolouration. Consequently, the treatment was performed at lower dye concentration and in the presence of chloride ion: 0.1g/L dye (which corresponds to the average residual dye in the industrial effluent) and 0.3g/L NaCl (to simulate the tap water content). In all cases, solutions were hydrolyzed previously to the electrochemical treatment, with the addition of NaOH and the solution was heated at 80°C for 2h. The final pH was approximately 12. Sodium sulphate was added to achieve the industrial effluents conductivity (35mS/cm).

2.4. Electrochemical treatment

The main difference between the two cell designs was the stirring mode, which affected the mass transfer conditions. The batch recirculation mode design (BRC) was a plug-flow reactor while the simple batch mode (SBC) was a simple tank with magnetic stirring. These two designs were selected due to their simplicity and feasibility of industrial implantation.

2.4.1. Batch recirculation mode cell design

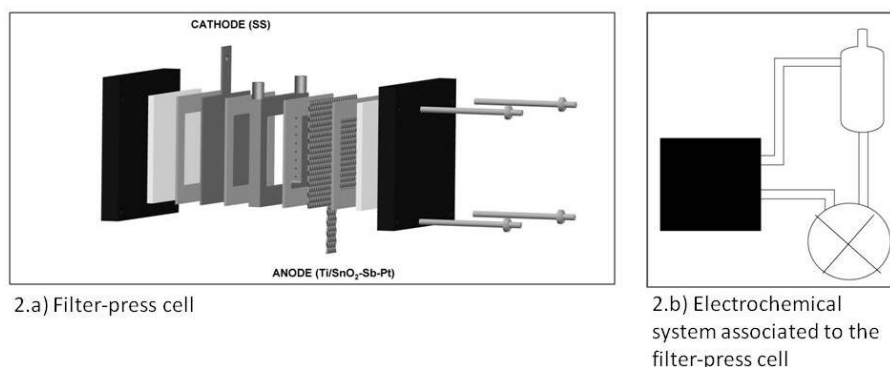


Figure 2. Filter-press cell design: a) Filter-press cell. b) electrochemical system showing the sample recipient, Cell (in black) and pump.

The electrolysis of hydrolyzed dyes in alkaline aqueous solutions were carried out in a batch recirculation mode cell where the effluent deposit was separated from the electrolysis reactor. They were connected with a pump as it is showed in Figure 2. The treated effluent was recirculated to the deposit continuously in a closed circuit.

The treated volume was 0.45L in all cases and all the tests were carried out under galvanostatic conditions with a power supply (Grelco GVD310 0-30Vcc / 0-10A). The applied current density was $125\text{mA}/\text{cm}^2$ until their total decolouration. The doped SnO_2 electrode (Ti/ SnO_2 -Sb-Pt) was selected for this part of the work. The electrodes area was 48.8cm^2 , and the recirculation flow was $5.6\text{L}/\text{min}$.

2.4.2. Simple batch mode cell

The synthetic effluents were treated in an undivided electrolytic cell as it is showed in Figure 3.

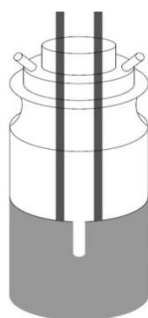


Figure 3. Batch cell (electrodes in black).

The volume treated was 2L in all cases and all the tests were also carried out under galvanostatic conditions with a power supply (Grelco GVD310 0-30Vcc / 0-10A). The stirring rate was 300rpm. The applied current density was $125\text{mA}/\text{cm}^2$ in the cell design study and $169\text{mA}/\text{cm}^2$ in the electrodes material study. In both cases, the treatment was carried out until the total decolouration of the effluent. The doped SnO_2 electrodes (Ti/ SnO_2 -Sb-Pt) were used in both studies and the electrode made of Ti/Pt was only used in the second study. The electrode area of Ti/Pt electrode was 59.3cm^2 .

2.5. Analysis and instruments

2.5.1. Spectroscopy analysis

The decolouration process was studied by UV-visible spectroscopy analysis. The initial dyes absorbance (Abs_0) was compared with the absorbance during the treatment (Abs_t). The absorbance was measured at the visible maximum dye absorption wavelength (600nm for RB5, 416nm for PY, 545nm for PC and 606nm for PN). Samples were analyzed during the electrochemical treatment each 5min and the decolouration evolution was reported in percentage (see equation 1).

$$(1) \quad D(\%) = (\text{Abs}_0 - \text{Abs}_t) * 100 / \text{Abs}_0$$

Absorbance measurements were carried out with a UV-Vis spectrophotometer (Shimadzu UV-2401 PC).

Dye absorbance has a linear behaviour versus the dye concentration as it is showed in Lambert Beer equation (2):

$$(2) \quad \text{Abs} = l \cdot \epsilon \cdot \text{conc.}$$

2.5.2. Kinetic evolution

As it is known, the organic pollutant abatement can be treated following pseudo-first order kinetics [33]. In accordance to previous studies [34], the dyes degradation really follows a pseudo-first order reaction with an electrochemical treatment. The decolouration rate constants (K_d) were calculated from the slope of semilogarithmic absorbance versus exposition time (t) or the specific applied charge (Q), accordingly with the kinetic equations (3-5):

$$(3) \quad -\ln (\text{Abs}_t / \text{Abs}_0) = k_d \cdot t$$

$$(4) \quad -\ln (\text{Abs}_t / \text{Abs}_0) = k_d \cdot Q$$

Where:

$$(5) \quad Q[A \cdot h / L] = I \cdot (t_t - t_0) / \text{vol}$$

2.5.3. HPLC and UV-Visible analyses

The chromatogram and corresponding UV-Vis spectra corresponding to each peak were obtained using a Hitachi Elite Lachrom Chromatographic System with a diode array detector. The method selected for the separation was based on EN14362-2:2003/AC. The column used was Lichrospher 100 RP-18C with 5 μm packing. The mobile phase was composed by methanol (eluent A) and aqueous buffer solution NaH_2PO_4 - Na_2HPO_4 (eluent B). The flow rate was $1\text{mL} \cdot \text{min}^{-1}$ at 298K and the injection volume was 80 μL .

Initially, the gradient elution for PY started with 15% A – 85% B, and it was progressively modified to 30% A – 70% B during 10min.

The gradient elution for RB5 was 0% A – 100% B initially (2min), and then it was gradually modified to 100% A – 0% B in 20min.

2.5.4. CGMS analysis

In order to evaluate the possible generation of volatile halogenated compounds, a GCMS method was used for the identification of 23 halogenated compounds. An Internal Standard (IS), p-bromofluorobenzene, was selected and used for the quantification of all these compounds.

The gas chromatography analyses were carried out in a Shimadzu QP 2010 (GCMS) system with a Mass Spectrum detector. The sample injection was carried out by a headspace technique, where 15mL of the sample was heated to 80°C for 45min in a 20mL vial, the vial was sealed with silicone/PFTE septum and 1mL of gas was injected to the CGMS. The injection temperature was

200°C. The chromatography program started at 35°C during 10min, the gradient rate was increased in 4°C/min until the final temperature at 150°C, remaining at this temperature for 10min. A TRB-624 column (length: 30m, internal diameter: 0.25mm, packing: 1.4µm) was used. The carrier gas was Helium with the column flow rate of 0.95mL/min.

The identification of halogenated compounds was performed using Nist 147, Nist 27 and Wiley 229 as reference libraries. Compounds, detections limits and the retention times are listed in Table 2.

Table 2. Volatile compounds selected for the GCMS analysis: retention time and detection limit.

Compound	CAS number	D.L. (µg/L)	Retention time (min)
Bromomethane	74-83-9	10	2,50
Chloroethane	75-00-3	1,0	2,65
Trichlorofluoromethane	75-69-4	2,5	3,00
1,1- Dichloroethene	75-35-4	2,5	3,86
Dichloromethane	75-09-2	1,0	4,90
1,1-Dichloroethane	75-34-3	2,5	6,55
Trichloromethane	67-66-3	1,0	9,69
1,1,1-Trichloroethane	71-55-6	2,5	10,07
Tetrachloromethane	56-23-5	2,5	10,63
Benzene	71-43-2	2,5	11,67
1,2-Dichloroethane	107-06-2	10	12,02
Trichloroethene	79-01-6	1,0	14,29
Bromodichloromethane	75-27-4	5	16,52
c-1,3-Dichloropropene	10061-01-5	10	18,22
Tetrachloroethene	127-18-4	1,0	21,03
Dibromochloromethane	124-48-1	10	22,32
Chlorobenzene	108-90-7	1,0	24,32
Ethyl-benzene	100-41-4	1,0	24,82
Tribromomethane	75-25-2	10	27,45
1-Bromo,3-Fluorobenzene	1073-06-9	2,5	28,61
1,3-Dichlorobenzene	541-73-1	1,0	32,48
1,4-Dichlorobenzene	106-46-7	0,5	32,85
1,2-Dichlorobenzene	95-50-1	0,5	34,17

The quantitative analysis was carried out by using the equation 6:

$$(6) \quad \text{Concentration}_c = (\text{Area}_c * \text{Concentration}_{IS}) / (\text{Area}_{IS} * R_f)$$

Where R_f is the response factor specific for each compound. It corresponds to the rate between the chromatographic response of the Internal Standard (1-bromo, 3-fluorobenzene) and the halogenated compound detected.

3. RESULTS AND DISCUSSION

3.1. Influence of the cell design

A comparison of effluents decolouration was carried out using the BRC and SBC cells. In both cases, the effluents were prepared as it is described in section 2.3, the concentration of dyes was 0.8g/L and sodium sulphate was added until the conductivity value was 35mS/cm. The treatment was carried out with the doped SnO₂ electrodes (Ti/SnO₂-Sb-Pt) and the current density was 125mA/cm².

3.1.1. Dyes decolouration.

The treated volume in the SBC reactor (2L) was higher than in the BRC design (0,45L). For that reason, the decolouration studies were represented as a function of the specific applied charge (Q) which is a normalised parameter respect to the volume. Due to the similar results obtained in both cell designs, the decolouration evolutions of the two selected dyes were represented for the SBC reactor in Figure 4. The total decolouration (>95%) was obtained.

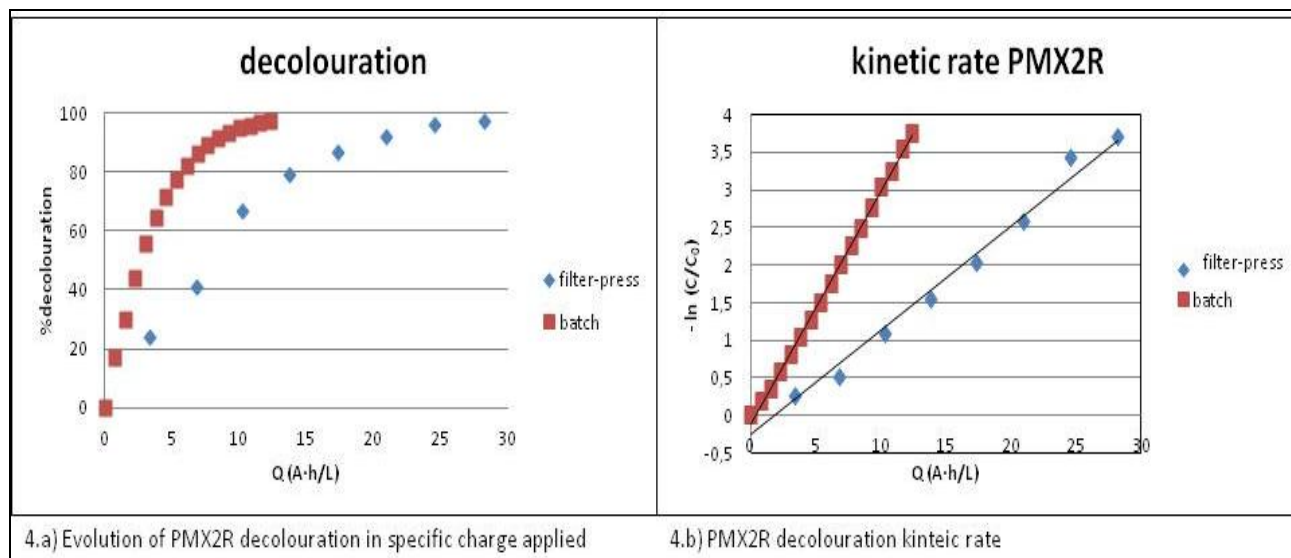


Figure 4. Decolouration of PMX2R dye in the two cells: filter-press and batch. Electrolysis conditions: 0.8g/L of dye, 15g/L of electrolyte Na₂SO₄, 125mA/cm² of current density. a) Percentage of decolouration versus the specific applied charge. b) Decolouration kinetic rate.

The decolouration kinetic rates values in both cell designs are shown in Table 3 for the two dyes studied.

Table 3. decolouration kinetic rate values

	Kd ($A^{-1}h^{-1}L$) batch recirculation cell	R^2	Kd ($A^{-1}h^{-1}L$) simple batch cell	R^2
PY	0.09	0.968	0.11	0.977
RB5	0.24	0.997	0.24	0.999

The RB5 kinetics is equal in both cells and PY kinetics is only slightly slower in the BRC. Due to the similar decolouration evolutions in both cell designs for dyes RB5 and PY, it can be concluded that the stirring mode is not a determinant factor on the dyes decolouration results.

Between the two dyes, the differences on their kinetic rates can be attributed to their different molecule structure. The kinetic rate is increased when the molecular structure is simpler. Both dyes have two azo chromophore groups to be degraded, so the difference between their decolouration rates is attributed to the rest of their molecular structure. PY kinetic rate is the slowest because it has more aromatic rings in its structure than RB5.

From the point of view of industrial application, both cells could achieve the full effluent decolouration and the design choice will be more dependent of factors such as cost, effluent volume or available space rather than the colour removal yield.

3.1.2. HPLC-DAD analysis

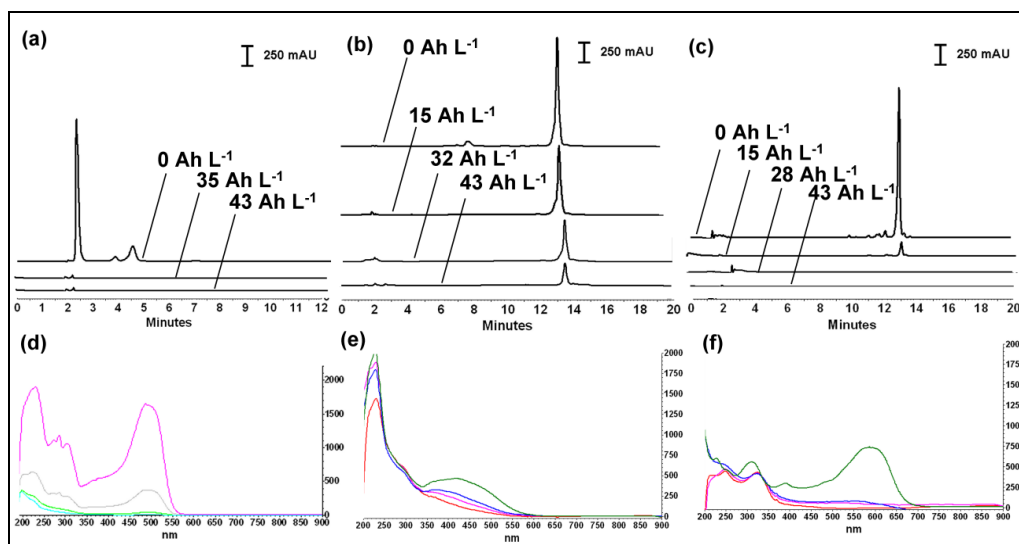


Figure 5. PMX2R, PY and RB5 decolouration with the following electrolysis conditions: 0.8g/L dye, 15g/L Na_2SO_4 , and $125mA/cm^2$ of specific applied charge. a) PMX2R chromatogram at different specific applied charges (retention time: 2.2min). b) PY chromatogram at different specific applied charges (retention time: 13.9min). c) RB5 chromatogram at different specific applied charges (retention time: 13.5min). d) PMX2R spectrum at different specific applied charges (maximum absorbance wavelength: 486nm). e) PY spectrum at different specific applied charges (maximum absorbance wavelength: 416nm). f) RB5 spectrum at different specific applied charges (maximum absorbance wavelength: 600nm).

The two dyes degradation study was carried out on the samples collected from the BRC and they were analyzed by HPLC-DAD. (Figure 5).

Figures 5a and 5c show the HPLC chromatograms, and in Figures 5b and 5d are plotted the UV-Visible spectra. The maximum peaks in the chromatograms with the retention time of 13.9min (5a) and 13.5min (5c) corresponded to the hydrolyzed PY and RB5 dyes respectively. The decreasing peaks with the increasing specific applied charge indicate the dye removal. These decreasing areas demonstrate that the dye chromophore group (azo group) is being degraded, and no additional peaks are detected at these wavelengths during the electrolysis.

In order to corroborate the dyes decolouration, Figures 5b and 5d shows the UV-visible spectra evolution which were plotted for the two studied dyes at several specific applied charges. The maximum absorbance wavelengths were 416nm and 600nm for PY and RB5 respectively (see Figures 5b and 5d). These figures confirmed dyes degradation because the absorbance band was decreasing with the specific applied charged.

A.I. del Rio et al. [20] carried out a mechanism study with this kind of dyes, and noticed that a peak at 250nm was observed after 2min of treatment (in the UV spectrum region) which corresponds to an intermediate generated during the electrochemical treatment with aromatic structure and high oxidation state.

3.2. Influence of electrode material

A comparison of effluents decolouration with the doped electrodes made of Ti/SnO₂-Sb-Pt and the electrodes made of Ti/Pt was carried out in the SBC. The effluents studied were prepared as described in section 2.3. Dyes concentration was 0.1g/L; sodium sulphate was added until 35mS/cm conductivity and also a 0.3g/L of sodium chloride was added to simulate the industrial conditions (it corresponds to the tap water content). The treatment current density was 169mA/cm².

This study was carried out using the SBC because the electrodes are visible and they are in the same recipient than the whole solution, so their tracing is more feasible. The comparison study was initiated with the two dyes previously studied (RB5 and PY), but due to their different behaviour, the study was extended to two additional dyes (PN and PC).

3.2.1. Dyes decolouration.

The decolouration evolution of the four selected dyes with the two types of electrodes is represented in Figure 6. It can be seen that, in all cases, 90% decolouration was achieved, although the doped SnO₂ electrode (Ti/SnO₂-Sb-Pt) was slower than the electrode made of Ti/Pt because a higher specific applied charge was required to achieve the same decolouration. The corresponding kinetic rates are listed in Table 4.

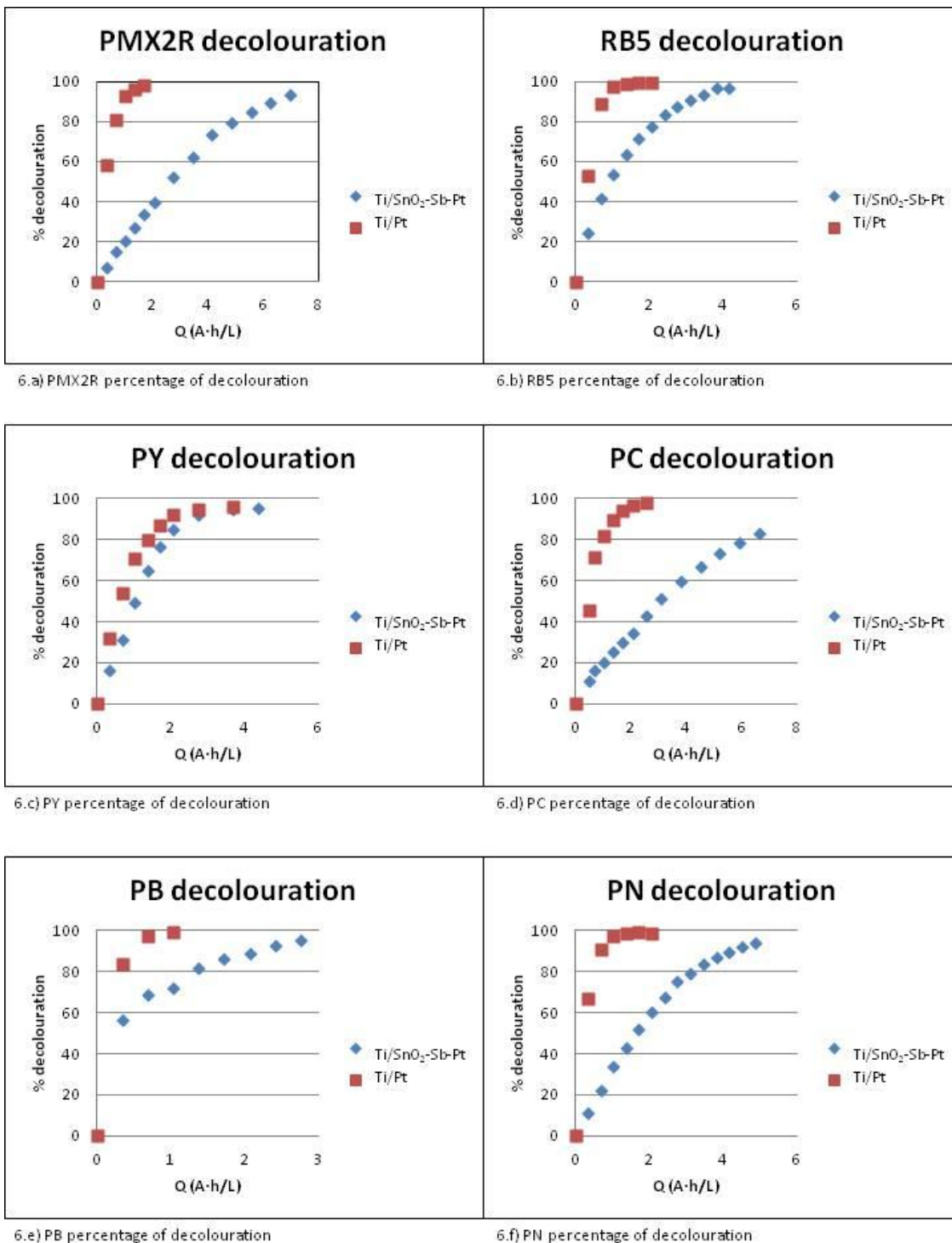


Figure 6. Decolouration evolution of the 6 selected dyes with the two types of electrodes.

According to Table 4, the decolouration rate with the Ti/Pt electrode is about 4.5 times higher than with the Ti/SnO₂-Sb-Pt electrode in the presence of NaCl as electrolyte. The different trends observed in Table 4 can be attributed to the different nature of the electrodes surface and, therefore, to the different mechanism for $\cdot\text{OH}$ radicals generation.

Regarding to the different mechanism for $\cdot\text{OH}$ radicals generation in the absence of chloride, it is known, from the data previously published [35, 36], that Pt behaves as an active anode due to its high electrocatalytic activity towards the oxygen evolution reaction (OER). Taking into account the model proposed by Comninellis et al. [37-41], the dye and its intermediates undergo a selective degradation. This is the result of the low concentration of adsorbed $\cdot\text{OH}$ radicals (that is, oxygen active sites) on the surface of Pt, which implies a low oxidation power towards the dyes/intermediates and, in consequence, gives a partial oxidation of these compounds.

Table 4. Kinetic rates of the 6 studied dyes, with the two electrode materials.

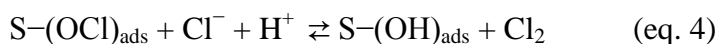
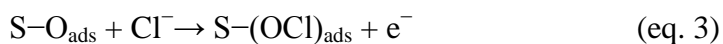
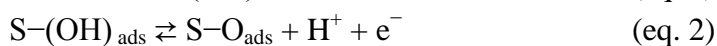
Dye	K_1 : {Ti/Pt} Kinetic rate ($\text{A}^{-1}\text{h}^{-1}\text{L}$)	R^2	K_2 : {Ti/SnO ₂ -Sb-Pt} Kinetic rate ($\text{A}^{-1}\text{h}^{-1}\text{L}$)	R^2	K_1/K_2	K_1/K_2 Average
RB5	2.94	0.992 7	0.77	0.997 1	3.81	
PY	1.04	0.998 4	1.02	0.993 8	1.02*	4.49*
PN	3.01	0.994 3	0.68	0.998 5	4.46	
PC	1.38	0.999 8	0.27	0.996 2	5.19	

*The PY K_1/K_2 value has not been considered in the K_1/K_2 average due to its different behaviour with respect to the other dyes.

On the contrary, the nature of the non-active Ti/SnO₂-Sb-Pt anodes makes them prone to present a high concentration of $\cdot\text{OH}$ radicals on its surface. In this case, the electrode must comply with an essential condition: the rate of $\cdot\text{OH}$ formation must be far much faster than the rate of oxygen transition into the oxide lattice (since this oxygen transition corresponds to active oxide film anodes behaviour). Consequently, the electrochemical behaviour of Ti/SnO₂-Sb-Pt and Ti/Pt electrodes differs quite a lot.

However, in the presence of chloride the behaviour of both anodes (Ti/SnO₂-Sb-Pt and Ti/Pt) is clearly modified. If we compare the results showed in Table 3 (without chloride) with the ones displayed in Table 4 (with chloride), it is obvious that the dyes degradation is strongly improved by using an inorganic mediator like “active chlorine”.

In fact, the amount of $\cdot\text{OH}$ radicals play an important role on the generation of active chlorine during the electrolyses. Different mechanisms of chlorine generation have been proposed by several authors. Some of them were chronologically reviewed by S. Trasatti [42] who concluded that the most realistic mechanism was based on the adsorption of oxychloro-radicals. Thus, the reaction mechanism for chlorine generation takes into account the acid base equilibrium at the surface as the first step of the chlorine generation mechanism and it can be represented according to equations 1-5 [42, 43],



where S corresponds to the active sites of the electrode surface.

Following to these papers, lots of works have been published where different substrates such as glucose [44, 45], oxalic acid [46], tannery wastewaters [47], thiourea dioxide [48] or several kinds of textile wastewater (even containing azo dyes) [35, 49, 50] were investigated in the presence of NaCl as electrolyte and Ti/Pt as anode. On the other hand, there are also several works where anodes like Ti/SnO₂-Sb-Pt have been employed in the presence of NaCl in order to degrade organic compounds such as phenolic compounds [51-53], tannery wastewaters [54, 55] or textile wastewaters [53, 56, 57].

Taking into account these considerations, the higher decolourisation rate of Ti/Pt electrodes versus the Ti/SnO₂-Sb-Pt electrode shown in Table 4 could be attributed to their different electrocatalytic activity towards the reaction of chlorine generation. In this sense, different works from literature have demonstrated that the formation of chlorine is far much catalysed by Ti/Pt electrodes than by Ti/SnO₂-Sb-Pt ones [58, 59]. Moreover, Bonfatti et al. confirmed the great dependence of the degradation process on chloride concentration when Ti/Pt was used as anode [44, 45]. According to their work, the presence of a relatively small amount of chloride ions seems to inhibit the OER, causing an increase of the anode potential and, therefore, a higher reactivity of adsorbed hydroxyl and oxychloro radicals. In this work, the concentration of NaCl was 0.3 g L⁻¹ which could be considered a low value. In addition to this, Panizza et al. demonstrated that the presence of chloride avoided the formation of a polymeric film on the Ti/Pt anode surface. Obviously, this fact improved the performance of these electrodes for the treatment of industrial effluents containing several polyaromatic compounds [60]. Furthermore, with regard to this film appeared on the Pt surface, Martínez-Huitle et al. [46] have also stated that the use of chlorides for the degradation of organic compounds changes the stoichiometry and microstructure of this film which inhibits the OER and favours the degradation process. Moreover, the electrogeneration of strong oxidants such as HClO, ClO⁻ and oxychloro compounds, as suggested in Pourbaix diagrams, is also a key factor. Therefore, it is obvious from the above considerations that the performance of Ti/Pt electrodes can be significantly improved in the presence of NaCl. On the contrary, the Ti/SnO₂-Sb-Pt electrodes are affected by the presence of chloride to a certain extent. In this sense, it should be taken into account that chloride ions are contained in all the industrial wastewater, and its effect should be taken under consideration.

Finally, it must be underlined that in the case of PY a different behaviour was obtained. The PY has the same decolouration rate in both studies which indicate that, in this particular case, the electrode material has no effect on the decolouration. Due to the different behaviour this dye, its K₁/K₂ value was not included in the K₁/K₂ average (Table 4).

This different behaviour of PY could be associated to the influence of the chemical structure on the degradation process. As reported by Martínez-Huitle and Brillas [18], the dependence of dyes degradation on their own chemical structure is not still well known. From Sanromán et al.

investigations [61], it could be concluded that not only the chemical structure influences the degradation process. The different substituents and their position also strongly affect the decolourisation process maybe because of the different estereochemical and resonance inductive effects [50]. The response of the dyes to the active chlorine mediated electrolyses is strongly affected by several variables such as pH or temperature which reflects the complexity of the degradation process. Therefore, more investigations are currently in progress in order to explain this behaviour in detail.

3.2.2. CGMS determination

Some electrode materials can catalyse the generation of halogenated volatile compounds, such as haloforms. For this reason, a sample was collected after each treatment and analyzed by GCMS with HS injection. The CGMS results plotted in Figure 7 show the gas chromatogram for RB5 reactive dye. Similar chromatograms were obtained for all studied dyes.

All the chromatograms exhibited two peaks. The first one corresponded to a volatile compound generated as a result of the electrochemical treatment (9.69min), and the second one was the Internal Standard p-bromofluorobenzene (28.61min). In all the studied cases, the treatment performed with the electrode made of Ti/Pt showed higher pollutant concentrations than the treatment carried out with the doped electrodes (Ti/SnO₂-Sb-Pt). This difference is appreciated in the Figure 7.

The first peak corresponded to the chloroform (trichloromethane), identified with a 94% of similarity, according to the instrument library Wiley 229 (Figure 8).

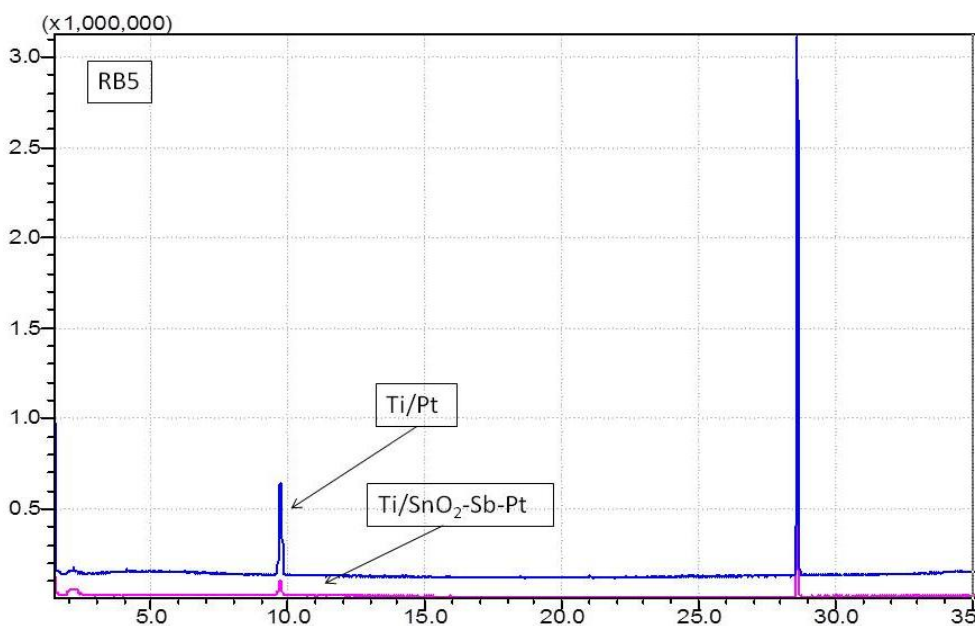


Figure 7. GCMS chromatogram with HS injection corresponding to RB5 decolouration (the chromatographic conditions are described in section 2.5.4). Detected compounds: chloroform (retention time 9.7min) and p-bromofluorobenzene (Internal Standard, retention time 28.6min).

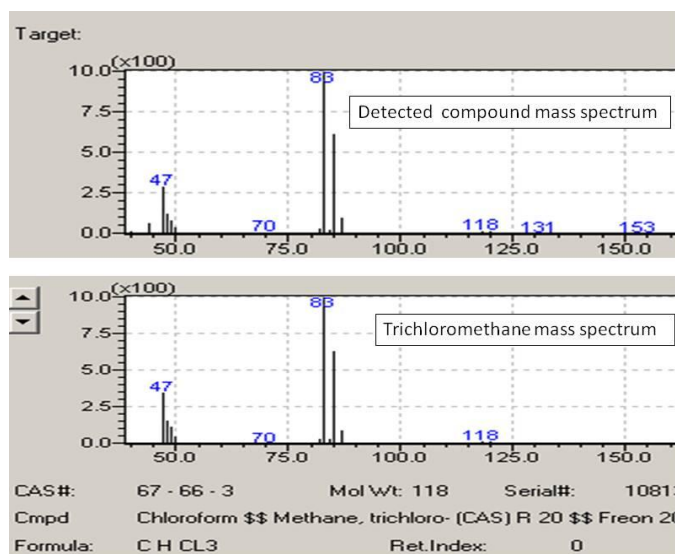


Figure 8. Mass Spectrum of the compound detected at retention time 9.7min (chromatogram in figure 7) and Mass Spectrum of chloroform.

In order to explain the differences on the chloroform concentration, the amount of active oxygen sites on the electrode surface prior to Cl₂ discharge should be taken into account. This is closely related to the different concentration of ·OH radicals on each electrode surface. Then, as indicated above, there is a higher accumulation of ·OH radicals on Ti/SnO₂-Sb-Pt surface which entails a higher reactivity.

Table 5. Treatment time to achieve 90% of decolouration and concentration of trichloromethane generated during this treatment, for the 6 studied dyes.

DYE	Trichloromethane concentration (ppm) to achieve 90% of decolouration.	
	Ti/Pt	Ti/SnO ₂ -Sb-Pt
RB5	0,78	0,12
PY	0,65	0,25
PC	1,66	0,24
PN	0,70	0,29

As a consequence of this, the dyes/intermediates undergo a non-selective transformation into CO₂ which can reasonably explain the lower concentration of chloro compounds obtained in this case. In fact, as reported by Stucki et al. [58, 59], the use of SnO₂-based anodes requires the use of about 5 times higher chloride concentrations to observe the same chlorination problems than with Pt electrodes. However, the formation of chlorinated compounds when the SnO₂-based electrodes are used should not be excluded. In this respect, it must be also indicated that some authors have demonstrated the formation of chlorinated compounds when performing the electrochemical treatment of a certain organic compound using a non-active electrode as anode [62]. Our GCMS analyses results

are in accordance with these previous findings. The amount of chloroform generated in each experiment is shown in Table 5. These values were calculated from the equation 6 (section 2.5.4), taking into account that the Internal Standard concentration was 1ppm and the R_f for the trichloromethane is 0.9594. It should be noticed that in all cases the amount of chloroform is very low.

The different concentration of the generated chlorocompounds is due to the different behavior towards the number of active oxygen sites, as above indicated. The only halogenated compound generated during the electrochemical treatment was trichloromethane, with a maximum concentration of 1.66ppm for the dye PC. This amount could be considered negligible taking into account that the dyeing effluents correspond only to the 10% of the total mill wastewater. That is to say, the dyeing effluent will be diluted 10 times and therefore, all the values showed in Table 5 will be much lower than 1ppm. In Catalonia, the decree 130/2003 establishes in 1ppm the maximum of chloroform allowed to be discharged. This limit can be different depending on the country and even, on the region.

In summary, it can be stated that the doped SnO_2 material electrode required a longer treatment time than the Titanium palatinate electrode to achieve the same decolouration level, which implied higher energy consumption. In contrast, the doped SnO_2 electrode generated a lower amount of volatile halogenated compounds (trichloromethane) than Ti/Pt electrode, which made them more suitable from the environmental point of view. Consequently, in the presence of low amounts of chloride, if the effluent is directly discharged to a river bed, the doped electrodes could be a better option, whereas Ti/Pt are more suitable when the dyeing effluent is further reused or treated in a biological plant.

4. CONCLUSIONS

An electrochemical treatment was applied in two undivided cells to decolourise four reactive dyes. Moreover two electrode materials were studied. The dyes degradation was followed by UV-Vis spectrophotometer determination and DAD-HPLC. CGMS analyses were also performed to identify and quantify the volatile compounds generated during the electrochemical treatment. From these results, the following differences between the two cell designs and the two electrode materials were established:

- The selected electrochemical technique (oxidation-reduction) demonstrated to be an effective method for the treatment of textile effluents (those which contains reactive dyes). All the cases studied achieved up to 90% of effluents decolouration.
- All the decolouration reactions followed a pseudo-first order kinetic.
- When comparing kinetic rates obtained in both cell designs, the two dyes studied presented similar decolouration evolutions. Therefore, the stirring mode is not a determinant factor in dyes decolouration results.
- The differences between the two dyes in their decolouration behaviour are attributed to their molecular structure. The dye with a simpler structure exhibited a higher decolouration kinetic rate.

- As expected, the electrode material was found to be an important factor on dyes degradation. In presence of chloride, the active anode made of Ti/Pt exhibit dyes degradation kinetic rates higher than the doped SnO₂ electrode (Ti/SnO₂-Sb-Pt).
- In contrast, the CGMS analysis showed that lower amounts of volatile halogenated compounds were generated when the doped SnO₂ electrode (Ti/SnO₂-Sb-Pt) was used.

ACKNOWLEDGEMENTS

The authors acknowledge the financial support of the Spanish Ministry of Economy and Competiveness (Projects CTM2007-66570-C02; CTM2010-18842-C02; CTM2011-23583) and ACC10-CIDEM/COPCA (Project J-04015).

References

1. M. Sala and M.C. Gutierrez, *Congress TexTehII*, Bucharest (2009).
2. A. Roessler and D. Crettenand, *Dyes Pigments*, 63 (2004) 29.
3. M. Weiss, *Am. Dyest. Rep.*, 67 (1978) 35.
4. E. Marte, *Text. Praxis Int.* 44 (1989) 737.
5. T. Robinson, G. McMullan, R. Marchant and P. Nigman, *Bioresources Tech.*, 77 (2001) 247.
6. N. Meksi, M. Kechida and F. Mhenni, *Chem. Eng. J.*, 131 (2007) 187.
7. D. Thetford and A.P. Chorlton, *Dyes Pigments*, 61 (2004) 49.
8. U. Baumgarte, *Melliand Textilberichte*, 68 (1987) 189.
9. E. Forgacs, T. Cserhati and G. Oros, *Environ. Int.*, 330 (2004) 953.
10. S.M. Burkinshaw, S.N. Chevli and D.J. Marfell, *Dyes Pigments*, 45 (2000) 65.
11. S.M. Burkinshaw, K. Lagonika and D.J. Marfell, *Dyes Pigments*, 58 (2003) 157.
12. S.M. Burkinshaw and K. Lagonika, *Dyes Pigments*, 69 (2006) 185.
13. M. Bozic and M. Kokol, *Dyes Pigments*, 76 (2008) 299.
14. M.C. Gutierrez and M. Crespi, *J. Soc. Dyes Colourist.*, 115 (1999) 342.
15. M.M. Naim and Y.M. El Abd, *Separ. Purif. Meth.*, 31 (2002) 171.
16. A.B. dos Santos, F.J. Cervantes and J.B. van Lier, *Bioresources Tech.*, 98 (2007) 2369.
17. C.A. Martinez-Huitle and S. Ferro, *Chem. Soc. Rev.*, 35 (2006) 1324.
18. C.A. Martin-Huile and E. Brillas, *Appl Catal B Environ.*, 87 (2009) 105.
19. T. Robinson, G. McMullan, R. Marchant and P. Nigman, *Bioresources Tech.*, 77 (2001) 247.
20. A.I. del Rio, J. Molina, J. Bonastre and F. Cases, *J. Haz. Mat.*, 172 (2009) 187.
21. A.I. del Rio, J. Molina, J. Bonastre and F. Cases, *Chemosphere*, 75 (2009) 1329.
22. A.I. del Rio, J. Fernandez, J. Molina and J. Bonastre, F. Cases, *Electrochim. Acta*, 55 (2010) 7282.
23. P.A. Carneiro, M.E. Osugi, C.S. Fugivara, N. Boralle, M. Furlan and M.V.B. Zanoni, *Chemospher.*, 59 (2005) 431.
24. G.A.R. Oliveira, E.R.A. Ferraz, F.M.D. Chequer, M.D. Grando, J.P.F. Angeli, M.S. Tsuboy, J.C. Marcarini, M.S. Mantovani, M.E. Osugi, T.M. Lizier, M.V.B. Zanoni and D.P. Oliveira, *Mutat. Res.: Genet. Toxicol. Environ. Mutagen.* (2010) doi:10.1016/j.mrgentox.2010.09.001
25. P.A. Carneiro, G.A. Umbuzeiro, D.P. Oliveira and M.V.B. Zanoni, *J. Hazard. Mater.*, 174 (2010) 694.
26. H. Zollinger, *Color Chemistry – Synthesis, Properties and Applications of Organic Dyes and Pigments*. V.C.H Publishers, New York, 1991.
27. C.C.I. Guaratini and M.V.B. Zanoni, *Quim. Nova*, 23 (2000) 71.
28. F. Vicent, E. Morallón, C. Quijada, J.L. Vázquez, A. Aldaz and F. Cases, *J. Appl. Electrochem.*, 28 (1998) 607.

29. F. Montilla, E. Morallón, A. De Battisti, S. Barison, S. Daolio and J.L. Vázquez, *J. Phys. Chem. B*, 108 (2004) 5036.
30. F. Montilla, E. Morallón, A. De Battisti, A. Benedetti, H. Yamashita and J.L. Vázquez, *J. Phys. Chem. B*, 108 (2004) 5044.
31. F. Montilla, E. Morallón, A. De Battisti and J.L. Vázquez, *J. Phys. Chem. B*, 108 (2004) 15976.
32. A.I. del Rio, J. Fernández, J. Molina, J. Bonastre and F. Cases, *Desalination*, 273 (2011) 428.
33. F. Torrades, J.A. Garcia-Hortal and L. Núñez, *Coloration Tech.*, 124 (2008) 370.
34. M. Riera-Torres and M.C. Gutierrez, *Chem. Eng. J.*, 156 (2010) 114.
35. V. López-Grimau and M.C. Gutiérrez, *Chemosphere*, 62 (2006) 106.
36. S. Hattori, M. Doi, E. Takahashi, T. Kurosu, M. Nara, S. Nakamatsu, Y. Nishiki, T. Furuta and M. Iida, *J. Appl. Electrochem.*, 33 (2003) 85.
37. Ch. Comminellis, *Electrochim. Acta*, 39 (1994) 1857.
38. Ch. Comminellis and E. Plattner, *Chimia*, 42 (1988) 250.
39. Ch. Comminellis and C. Pulgarin, *J. Appl. Electrochem.*, 21 (1991) 1403.
40. Ch. Comminellis, *Gas, Wasser, Abwasser*, 11 (1992) 792
41. Ch. Comminellis and C. Pulgarin, *J. Appl. Electrochem.*, 23 (1993) 108.
42. S. Trasatti, *Electrochim. Acta*, 32 (1987) 369.
43. R.G. Erenburg, *Elektrokhimiya*, 20 (1984) 1602.
44. F. Bonfatti, S. Ferro, F. Lavezzo, M. Malacarne, G. Lodi and A. De Battisti, *J. Electrochem. Soc.*, 147 (2000) 592.
45. F. Bonfatti, A. De Battisti, S. Ferro, G. Lodi and S. Osti, *Electrochim. Acta*, 46 (2000) 305.
46. C.A. Martínez-Huitle, S. Ferro and A. De Battisti, *Electrochem. Solid State Letters*, 8 (2005) 35.
47. A.G. Vlyssides and C.J. Isreilides, *Environ. Pollut.*, 97 (1997) 147.
48. L. Szpyrkowicz, C. Juzzolino, S. Daniele and M. Dante De Faveri, *Catal. Today*, 66 (2001) 519.
49. A.G. Vlyssides, M. Loizidou, P.K. Karlis, A.A. Zorpas and D. Papaioannou, *J. Hazard. Mater. B*, 70 (1999) 41.
50. A. Sakalis, K. Mpoulmpasakos, U. Nickel, K. Fytianos and A. Voulgaropoulos, *Chem. Eng. J.*, 111 (2005) 63.
51. A.M. Polcaro, S. Palmas, F. Renoldi and F. Mascia, *J. Appl. Electrochem.*, 29 (1999) 147.
52. M. Zhou, Q. Dai, L. Lei, C. Ma and D. Wang, *Environ. Sci. Technol.*, 39 (2005) 363.
53. X. Chen, F. Gao and G. Chen, *J. Appl. Electrochem.*, 35 (2005) 185.
54. M. Panizza and G. Cerisola, *Environ. Sci. Technol.*, 38 (2004) 5470.
55. L. Szpyrkowicz, S.N. Kaul, R.N. Neti and S. Satyanarayan, *Water Research*, 39 (2005) 1601.
56. L.S. Andrade, L.A. M. Ruotolo, R. C. Rocha-Filho, N. Bocchi, S.R. Biaggio, J. Iiesta, V. García-García and V. Montiel, *Chemosphere*, 66 (2007) 2035.
57. N. Mohan, N. Balasubramanian, C. Ahmed Basha, *J. Hazard. Mater.*, 147 (2007) 644.
58. S. Stucki, R. Kötz, B. Carcer and W. Suter, *J. Appl. Electrochem.*, 21 (1991) 99.
59. S. Stucki, R. Kötz and B. Carcer, *J. Appl. Electrochem.*, 21 (1991) 14.
60. M. Panizza, C. Bocca and G. Cerisola, *Water Research*, 34 (2000) 2601.
61. M.A. Sanromán, M. Pazos, M.T. Ricart and C. Cameselle, *Chemosphere*, 57 (2004) 233.
62. M. Panizza, M. Delucchi and G. Cerisola, *J. Appl. Electrochem.*, 35(2005) 357.